



Defect annihilation in heavy ion irradiated polycrystalline gold

Zahabul Islam ^a, Christopher M. Barr ^b, Khalid Hattar ^b, Aman Haque ^a

^a Department of Mechanical Engineering, The Pennsylvania State University, University Park, PA 16802, USA

^b Sandia National Laboratories, PO Box 5800-1058, Albuquerque, NM 87185, USA



ARTICLE INFO

Article history:

Received 25 August 2020

Received in revised form 13 September 2020

Accepted 14 September 2020

Available online 17 September 2020

Keywords:

Radiation damage

Recrystallization

Microstructure

In-situ Transmission Electron Microscopy

Electrical wind force

Shockley partial dislocations

ABSTRACT

In this study, we explore the interaction of electron wind force (EWF) with defects originating from ion irradiation in-situ inside a transmission electron microscope. Nanocrystalline gold specimens were self-ion irradiated to a dose of 5×10^{15} ions/cm² (45 displacement per atom) to generate a high density of displacement damage. We also developed a molecular dynamics simulation model to understand the associated atomic scale mechanisms. Both experiments and simulations show that the EWF can impart significant defect mobility even at low temperatures, resulting in the migration and elimination of defects in a few minutes. We propose that the EWF interacts with defects to create highly glissile Shockley partial dislocations, which makes the fast and low temperature defect annihilation possible.

© 2020 Elsevier B.V. All rights reserved.

1. Introduction

During irradiation, highly energetic particles (ions, neutrons, electrons) collide with atoms in materials, thereby generating various types of defects [1,2]. Considerable amount of efforts in the literature is dedicated on formation, structure and properties of defects [1,3]. Defect annihilation or microstructural control in irradiated materials is relatively less studied. The predominant mechanism for defect annihilation is thermal annealing [4], which involves high temperature. Electro-thermal effects are also known to control defects and microstructure. Electro-pulsing is a common approach, where the very small loading duration (tens of microseconds) applies intense electrical and thermal stimuli with minimal increase in overall temperature [5]. An intriguing analogy can be drawn with sever plastic deformation (SPD), where a steady state between defect generation and annihilation) is observed at low temperature T_{SPD} [6], even though the defect annihilation rate would imply a higher temperature if thermal annealing were the driving mechanism.

In this study, we propose that thermal vibration is not the only way to make defects mobile and introduce the electron wind force (EWF) as a non-thermal stimulant. When current is passed in metals, Joule heating and the EWF arise from lattice and defect scattering respectively. EWF arises due to defect scattering only since electron flow in the lattice is considered ballistic compared to

defects such as grain boundaries [7]. Thus, EWF is a mechanical force in nature, imparted to defective atoms during collision and momentum transfer by the electrons [8]. It is highly specific to defects since no such momentum transfer takes place in the crystalline region. We hypothesize that such high defect-specificity make it an efficient (fast and low temperature) driver for defect annihilation. In this study, we minimize Joule heating effects by suspending our 100 nm thick specimens on silicon beams with $20 \times 20 \mu\text{m}^2$ cross-section. Because they effectively act as massive heatsinks, the silicon beams develop a parabolic temperature profile in the specimen with the two ends at ambient and the middle section at highest temperature [9]. We exploit this temperature profile by restricting our investigation near the support regions only. Such thermal boundary condition driven decoupling of EWF and Joule heating has allowed us to study EWF effects on defects [10,11] with DC current.

2. Methods and materials

Gold film (about 500 nm thick) was irradiated normal to the surface with 1.5 MeV Au⁺ ions using the 6MV HVE Tandem accelerator at Sandia National Laboratories. The fluence was approximately 6.5×10^{15} ions/cm² and corresponding Stopping and Range of Ions in Matter (SRIM) calculated displacement per atom (dpa) profile is shown in Fig. 1a. After ion irradiation we used Ga⁺ Focused Ion Beam (FIB) based lift out technique to prepare nominally 100 nm thick, electron transparent specimens and

E-mail address: mah37@psu.edu (A. Haque).

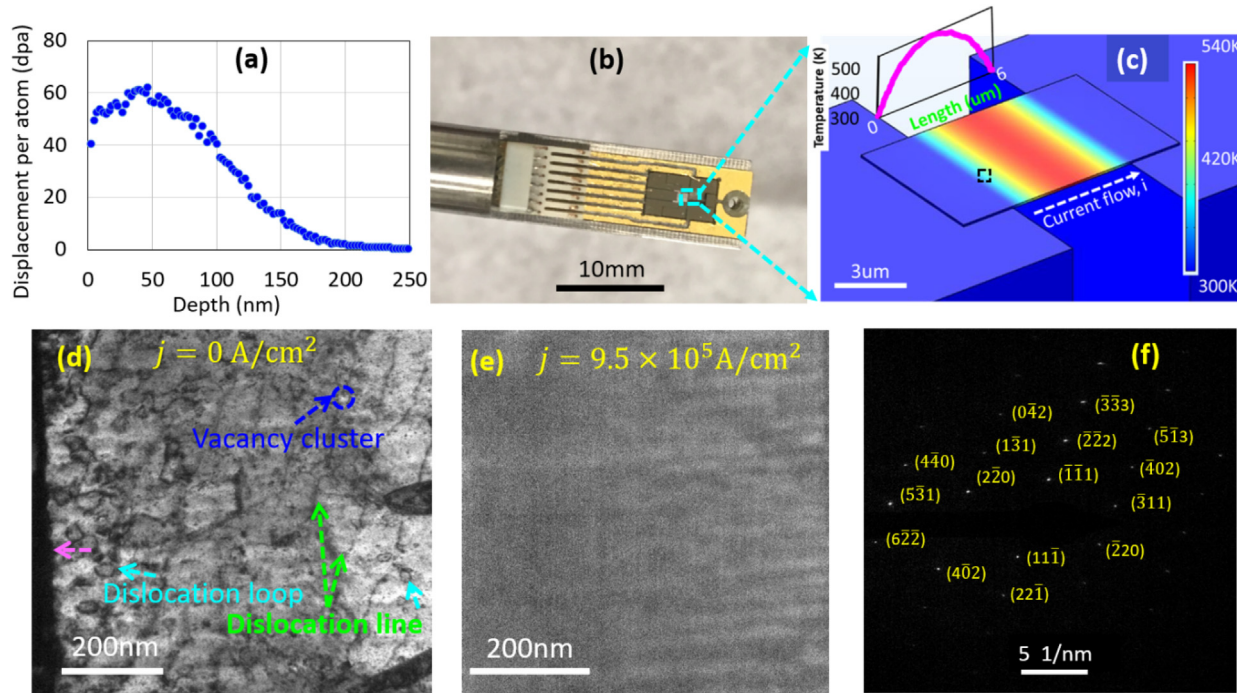


Fig. 1. (a) Displacement per atom (dpa) profile for irradiation dose of $6.5 \times 10^{15} \text{ ion/cm}^2$, (b) MEMS device mounted on in-situ TEM holder, (c) temperature profile obtained from electro-thermal simulation, (d) TEM BF image showing irradiation damage, (e) BF image showing dislocation annihilation at $9.5 \times 10^5 \text{ A/cm}^2$, and (f) SAED pattern after EWF annealing.

mounted them on an in-situ TEM holder (Fig. 1b). To complement the experiments, we performed molecular dynamics (MD) simulation to qualitatively investigate the atomic scale processes behind defect annihilation. Further details on experimental [10,11] and computational modeling [10] are available in the literature as well as the [Supplementary information](#). To perform EWF-based annealing, we passed DC current in finite steps of $0.5 \times 10^5 \text{ A/cm}^2$ while observing the low temperature region of the specimens inside the TEM. This is shown with the dotted box in Fig. 1c, where the massive heatsinks (electrodes) constrain the temperature around 300 K as indicated by a multi-physics simulation in COMSOL. This is significantly low compared to the thermal annealing temperature of 525 K [12]. For each current level, about 5 min hold time was allowed.

3. Results and discussion

Effect of EWF on defect mobility was visually observed around current density $\sim 5 \times 10^5 \text{ A/cm}^2$. We choose an individual grain located at the specimen edge to investigate specific types of defects and their annihilation mechanism under EWF as shown by TEM bright field (BF) image. Fig. 1d shows the irradiation induced dislocation lines (green color arrow), dislocation loops (cyan color arrow), and vacancy cluster (blue color circle) in a specimen. Fig. 1e clearly shows the same area transformed into a highly ordered crystal, corroborated by the selected area electron diffraction (SAED) pattern in Fig. 1f. BF images as shown in Fig. 1e indicates dislocations annihilation during EWF annealing. Further details are given in [Supplementary Fig. S1](#). The process is very rapid compared to thermal annealing. At this current density, it took less than 5 min to achieve a defect free single crystalline area where the temperature was constrained to the ambient.

To investigate how the EWF interacts with the defects and causes them to migrate towards sinks, we performed MD

simulations. Our extensive computational experiments suggest that the fundamental mechanism behind EWF based annealing is the splitting of defects into Shockley partial dislocations. Details of computational modeling and results are provided as [Supplementary information](#). Fig. 2a-c show our computational results for specimens containing two dislocations and vacancy clusters, while Fig. 2d-e are for one stacking fault tetrahedron (SFT) between two grain boundaries. For each case, we observed EWF induced dissociation into partial dislocations, which are highly mobile (through gliding motion) defects [13] that can be further swept by the EWF towards the defect sinks.

In low stacking fault energy materials, irradiation generates SFTs that are very difficult to remove below 873 K [14]. With EWF, we were able to annihilate SFTs at around ambient temperature as shown by Fig. 2d-f (computational) and Fig. 3 (experimental). Fig. 3a manifests high resolution TEM (HRTEM) bright field image with high density of SFTs (cyan color arrow and yellow color dotted triangle). Fig. 3b shows an atomic resolution image of a single SFT defect before the EWF processing. Surface induced SFT annihilation under the effect of EWF is shown in Fig. 3c. Such annihilations of SFT are marked by cyan color dotted arrow (Fig. 3c). At higher current densities, the SFT interacts with the GBs as shown in Fig. 3d to be subsequently absorbed by the GBs. This is the same location as in Fig. 3a and 3c. Such GB-SFT interaction has been shown in Fig. 3e with atomic resolution. Complete defects annihilation is observed at a current density of $9.5 \times 10^5 \text{ A/cm}^2$ and corresponding image is shown in Fig. 3f. MD simulation of SFT annihilation under EWF is shown in Fig. 2d-f. Here, the SFTs were computationally composed of stair-rod dislocations. The role of the EWF is to disintegrate them to Shockley partial dislocations, which migrate through the grain and subsequently become absorbed by the GBs (Fig. 2e). This is suggested by our dislocation density calculations showing diminishing stair-rod dislocations with simultaneous increase in the Shockley partials as indicated by Fig. 2f.

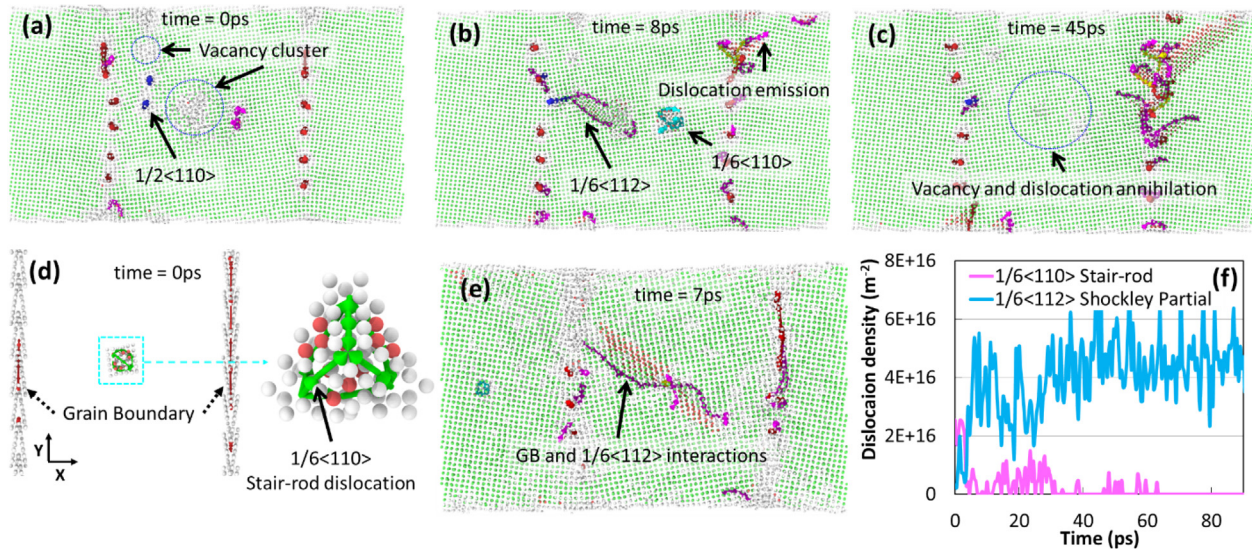


Fig. 2. Computational results on (a)-(c): Annihilation of dislocations and vacancy clusters, and (d)-(f): SFT annihilation under EWF.

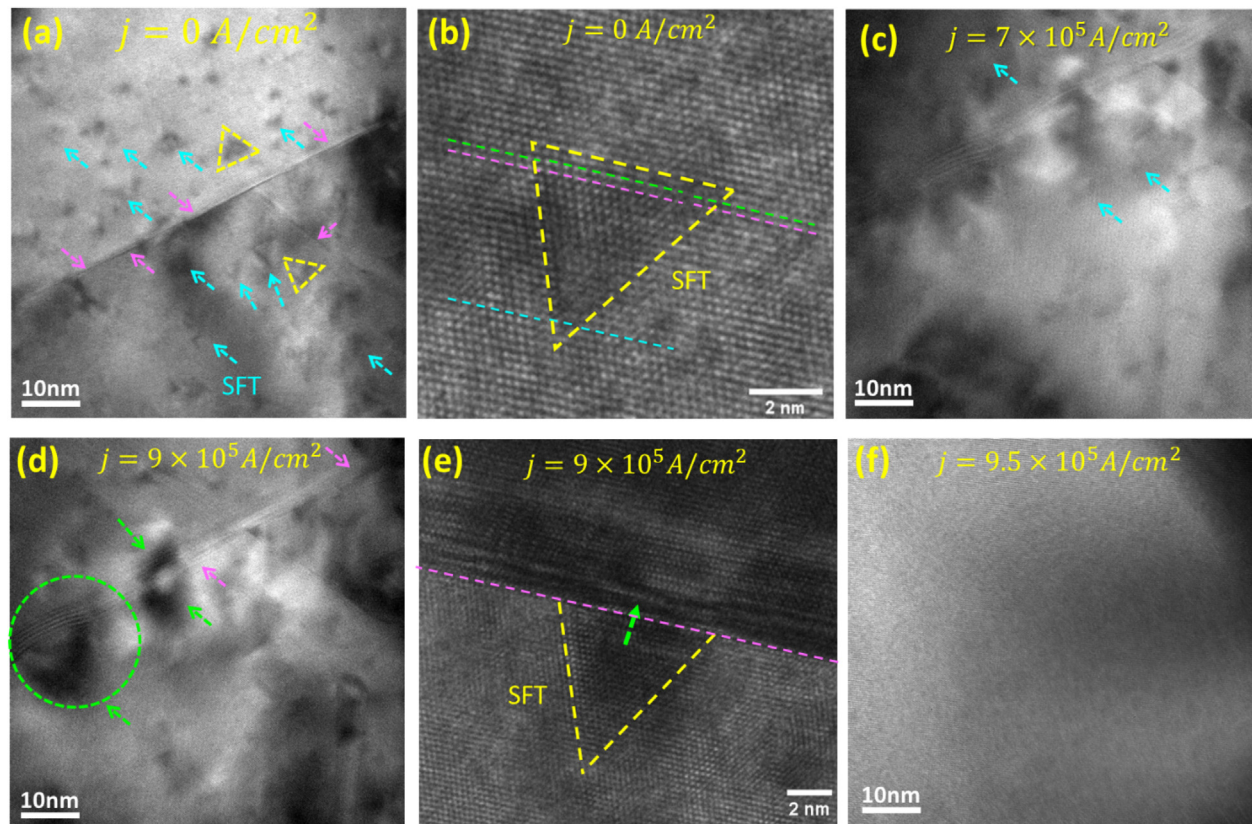


Fig. 3. HRTEM images of low temperature processing of irradiated materials: (a) defects in the irradiated sample before processing, (b) HRTEM image of SFT, (c) Surface induced annihilation of SFT at a current density of $7 \times 10^5 \text{ A/cm}^2$, (d) SFT-GB interaction at $9 \times 10^5 \text{ A/cm}^2$, (e) HRTEM image of SFT-GB interaction, and (f) After EWF annealing at $9.5 \times 10^5 \text{ A/cm}^2$.

4. Conclusion

Our study shows that the EWF interaction with defects such as dislocations and SFT can induce significant mobility even at room temperature. This non-thermal process is hypothesized with the help of computational results indicating generation of high density of glissile and reactive (with other defects) Shockley partial dislocations. Similar high mobility may govern the steady state defect

density in SPD. However, more work is needed to reconcile EWF and SPD phenomena because our specimens tend to grow larger crystal grains, whereas SPD tends to refine grains. An important feature of this process is the EWF is absent in non-defective regions, therefore the electrical energy input is specifically targeted towards the defective regions resulting in rapid, 'just in location' annihilation of defects.

CRediT authorship contribution statement

Zahabul Islam: Methodology, Investigation, Writing - original draft. **Christopher M. Barr:** Methodology, Software, Formal analysis. **Khalid Hattar:** Visualization, Investigation, Supervision. **Aman Haque:** Conceptualization, formal analysis, funding acquisition, methodology, project administration, writing (reviewing and editing).

Declaration of Competing Interest

The authors declare that they have no known competing financial interests or personal relationships that could have appeared to influence the work reported in this paper.

Acknowledgement

MAH acknowledges support from the National Science Foundation through award # CMMI 1760931. SNL work was performed, in part, at the Center for Integrated Nanotechnologies, an Office of Science User Facility operated for the U.S. Department of Energy (DOE) Office of Science. Sandia National Laboratories is a multi-mission laboratory managed and operated by National Technology and Engineering Solutions of Sandia, L.L.C., a wholly owned subsidiary of Honeywell International, Inc., for the U.S. Department of Energy's National Nuclear Security Administration under contract DE-NA-0003525. The views expressed in the article do not necessarily represent the views of the U.S. DOE, NSF or the United States Government.

Appendix A. Supplementary data

Supplementary data to this article can be found online at <https://doi.org/10.1016/j.matlet.2020.128694>.

References

- [1] G.S. Was, Fundamentals of Radiation Materials Science, Springer-Verlag, New York, 2017.
- [2] X.H. Zhang, K. Hattar, Y.X. Chen, L. Shao, J. Li, C. Sun, K.Y. Yu, N. Li, M.L. Taheri, H.Y. Wang, J. Wang, M. Nastasi, Radiation damage in nanostructured materials, *Prog. Mater Sci.* 96 (2018) 217–321.
- [3] L. Chen, L.Q. Li, H.R. Gong, J.L. Fan, W. Li, Irradiation effect on mechanical properties of tungsten from molecular dynamic simulation, *Mater. Lett.* 241 (2019) 27–30.
- [4] F. Ferroni, X.O. Yi, K. Arakawa, S.P. Fitzgerald, P.D. Edmondson, S.G. Roberts, High temperature annealing of ion irradiated tungsten, *Acta Mater.* 90 (2015) 380–393.
- [5] Y. Sheng, Y. Hua, X. Wang, X. Zhao, L. Chen, H. Zhou, J. Wang, C.C. Berndt, W. Li, Application of high-density electropulsing to improve the performance of metallic materials: mechanisms, microstructure and properties, *Materials* 11 (2) (2018).
- [6] B.B. Straumal, A.R. Kilmametov, Y. Ivanisenko, A.A. Mazilkin, O.A. Kogtenkova, L. Kurmaneva, A. Korneva, P. Zięba, B. Baretzky, Phase transitions induced by severe plastic deformation: steady-state and equifinality, *Int. J. Mater. Res.* 106 (7) (2015) 657–664.
- [7] H.B. Huntington, A.R. Grone, Current-induced marker motion in gold wires, *J. Phys. Chem. Solids* 20 (1–2) (1961) 76–87.
- [8] H.B. Huntington, Effect of driving forces on atom motion, *Thin Solid Films* 25 (2) (1975) 265–280.
- [9] M.T. Alam, M.P. Manoharan, M.A. Haque, C. Muratore, A. Voevodin, Influence of strain on thermal conductivity of silicon nitride thin films, *J. Micromech. Microeng.* 22 (4) (2012) 045001.
- [10] Z. Islam, H.J. Gao, A. Haque, Synergy of elastic strain energy and electron wind force on thin film grain growth at room temperature, *Mater. Charact.* 152 (2019) 85–93.
- [11] K.Z. Zahabul Islam, J. Robinson, A. Haque, Quality enhancement of low temperature metal organic chemical vapor deposited MoS₂: an experimental and computational investigation, *Nanotechnology* 30(Number (2019) 39).
- [12] I. Nashiyama, P.P. Pronko, K.L. Merkle, Annealing study of self-ion-irradiated gold by proton channeling, *Radiation Effects* 29 (2) (1976) 95–98.
- [13] W. Cai, V.V. Bulatov, J. Chang, J. Li, S. Yip, Dislocation core effects on mobility, *Dislocations in Solids* 12 (2004) 1–80.
- [14] B.N. Singh, S.I. Golubov, H. Trinkaus, D.J. Edwards, M. Eldrup, Review: Evolution of stacking fault tetrahedra and its role in defect accumulation under cascade damage conditions, *J. Nucl. Mater.* 328 (2–3) (2004) 77–87.